

Electron knock-on damage in hexagonal boron nitride monolayers

J. Kotakoski,¹ C. H. Jin,^{2,3} O. Lehtinen,¹ K. Suenaga,² and A. V. Krasheninnikov^{1,4}

¹Materials Physics Division, University of Helsinki, P.O. Box 43, 00014 Helsinki, Finland

²Nanotube Research Center, National Institute of Advanced Industrial Science and Technology (AIST), Tsukuba 305-8565, Japan

³Department of Materials Science and Engineering, Meijo University, Tenpaku-ku, Nagoya 468-8502, Japan

⁴Department of Applied Physics, Aalto University, P.O. Box 1100, 00076 Aalto, Finland

(Received 23 July 2010; published 7 September 2010)

We combine first-principles molecular-dynamics simulations with high-resolution transmission electron microscopy experiments to draw a detailed microscopic picture of irradiation effects in hexagonal boron nitride (*h*-BN) monolayers. We determine the displacement threshold energies for boron and nitrogen atoms in *h*-BN, which differ significantly from the tight-binding estimates found in the literature and remove ambiguity from the interpretation of the experimental results. We further develop a kinetic Monte Carlo model which allows to extend the simulations to macroscopic time scales and make a direct comparison between theory and experiments. Our results provide a comprehensive picture of the response of *h*-BN nanostructures to electron irradiation.

DOI: [10.1103/PhysRevB.82.113404](https://doi.org/10.1103/PhysRevB.82.113404)

PACS number(s): 61.80.Az, 31.15.es, 61.48.De

Isolated hexagonal boron nitride (*h*-BN) monolayer^{1,2} has a two-dimensional honeycomb structure similar to graphene³ with carbon atoms replaced by alternating boron and nitrogen atoms. Contrary to graphene, *h*-BN is a wide gap semiconductor due to ionic bonding between the atoms, with the potential to tune the electronic properties of *h*-BN-based systems by applying electric field to BN nanoribbons⁴ or by making hybrid C-BN materials.⁵ The first high-resolution transmission electron microscopy (HRTEM) studies⁵⁻⁷ of *h*-BN have revealed peculiar triangle-shaped multivacancy structures which have never been observed in graphene. Nitrogen termination of the edges has been suggested.⁶ These defects may govern the electronic and magnetic properties of *h*-BN systems^{4,8,9} while the knowledge of the precise mechanism of their formation is important for electron-beam engineering^{10,11} of such structures.

In an attempt to understand electron-beam damage in *h*-BN and to give an interpretation of the experiments, the formation energies of various defects in *h*-BN monolayers have been calculated.¹²⁻¹⁵ Negative charging has been argued to explain nitrogen termination of the multivacancy edges.^{14,15} However, electron deficiency rather than injection should be expected for atomically thin samples under the high-energy (~ 100 kV) electron beam¹⁶ in a HRTEM due to secondary electron emission. Moreover, as the defects are created under the beam, the evolution of the defects should be governed by knock-out probabilities instead of equilibrium thermodynamics. An early study¹⁷ addressed this issue within the framework of a tight-binding (TB) model. Nearly similar displacement thresholds (i.e., the minimum amount of kinetic energy that, when delivered to an atom in the system, results in the ejection of the atom away from the system) for boron and nitrogen were obtained, which has caused much confusion, because a strong asymmetry would be required to explain the experimental observations.^{6,7,15} Therefore, the mechanism of triangular defect formation and the chemical nature of the stable zigzag edge still remain unresolved.

In this work, to draw the microscopic picture of the production and evolution of defects in *h*-BN, we combine mul-

tiscale atomistic computer simulations with HRTEM experiments on electron irradiation of *h*-BN. Contrary to previous studies where single electron energy was used, we study the response of *h*-BN to irradiation at various acceleration voltages (80, 120, and 200 kV), which provides direct data on the dependence of defect production rate on electron energy. Using first-principles molecular-dynamics (MD) simulations, we calculate the knock-on displacement thresholds for boron and nitrogen atoms in the pristine structure and at different vacancy edges in various charge states. We extend our simulations to macroscopic times by kinetic Monte Carlo (KMC) method. The obtained threshold energies differ significantly from the TB results,¹⁷ and display a strong asymmetry for the values for boron and nitrogen. Our experimental and theoretical results show that the formation and evolution of the triangle-shaped multivacancies is governed by knock-on displacement rates, in contrast to the previously suggested explanations^{14,15} where charging effects and thermodynamics of the defects was emphasized. Overall, our results provide a comprehensive picture of the response of *h*-BN nanostructures to electron irradiation.

The *h*-BN samples used in our experiments were mainly few-layer nanosheets (for details on sample preparation, see Ref. 6). Of the multilayer structures, one layer was sputtered at a time with the electron beam, until monolayered areas were obtained for this study. The samples were checked under an aberration-corrected TEM (JEOL 2010F), which was operated at different acceleration voltages. We extended the TEM voltages used in previous *h*-BN studies up to 200 kV and repeated experiments at voltages of 80 kV and 120 kV, as was done in Refs. 7 and 6, respectively. The typical defect structures created at different voltages are presented in Fig. 1. The observed defects have distinguished sizes, the smallest being a monovacancy, and they all have exactly the same orientation, as in the earlier studies.^{6,7} The shape of the defects indicates that undercoordinated atoms of one species are knocked out more frequently under the electron beam. By estimating the number of sputtered atoms and comparing the ratios between the ejected three-coordinated B/N atoms and undercoordinated B/N atoms (assuming the first ejected

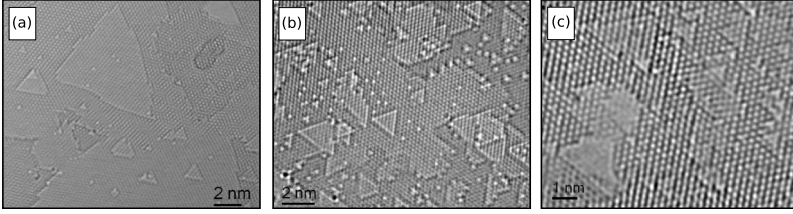


FIG. 1. Examples of the *h*-BN structures after an exposure to a TEM beam with different acceleration voltages: (a) 80 kV, (b) 120 kV, and (c) 200 kV.

atom is boron for each vacancy, see below), we notice that the thresholds for displacing undercoordinated atoms change when the vacancy structures grow. Our estimates indicate that the threshold drops by a factor of approximately 3 for B and about half of that for N. This effect is partly due to the stabilizing interaction between edge atoms in small vacancies.^{13,14} Moreover, at high vacancy concentrations narrow atomic bridges appear between vacancies. These areas become unstable under the electron beam, which may be interpreted as a drop in the threshold of the undercoordinated atoms.

In order to understand the mechanism of damage creation in a *h*-BN monolayer, we carried out atomistic computer simulations of energetic electron impacts onto *h*-BN monolayers. We used an approach similar to that of Ref. 17. However, instead of TB, we employed density-functional theory (DFT) MD as implemented in the VASP code.¹⁸ We used projector-augmented wave potentials¹⁹ to describe the core electrons, and the generalized gradient approximation²⁰ for exchange and correlation. To estimate the kinetic energy T needed to eject an atom (displacement threshold T_d) from the pristine system—in our case consisting of a 4×6 supercell—we carried out simulations in which we assigned T to one of the atoms in the structure with a velocity perpendicular to the sheet. Then, we increased T until the ejection of the atom occurred. Since one of the key issues we wanted to address with these calculations was the production of extended vacancy structures under the electron beam, we repeated the calculation for atoms at the edges of monovacancies (V_B and V_N) and nonvacancies (nine missing atoms; $V_{B_3N_6}$ and $V_{B_6N_3}$).

For the pristine structure, we obtained $T_d^B = 19.36$ eV and $T_d^N = 23.06$ eV for B and N, respectively. These values differ significantly from the earlier TB results (15 eV/14 eV for B/N).¹⁷ This discrepancy is likely due to inadequate description of the charge transfer in this binary system by the TB model. This point is supported by the fact that the TB values of 23 eV (Ref. 17) and 22.2 eV (Ref. 21) for displacing a C atom from graphene sheet (where no substantial charge transfer occurs) is much closer to our result of 22.03 eV obtained from first principles.

As discussed in Ref. 17, the theoretical values can be expected to be at least 10% higher than the experimental ones because only the ground-state dynamics is considered in the calculations. The beam-induced excitations may reduce the bonding energy of the atoms in the lattice, thus reducing the threshold energy. However, as the effect is expected to be systematic, we can assume that the obtained thresholds are overestimations, and simply correct for this by comparing the results to experiments. Assuming maximum energy transfer from the electron to a target atom,^{17,21,22} the

calculated T_d correspond to acceleration voltages of 88 kV/130 kV for B/N. Taking into account a 10% overestimation, the corresponding voltages would be approximately 79.5 kV and 118.6 kV, respectively. These results are in a very good agreement with the experiments in which only one type of monovacancies are seen both at 80 kV (Ref. 7) and 120 kV.⁶ Below, we will use the corrected values in further calculations to allow for a direct comparison between the experimental and theoretical acceleration voltages.

In the case of monovacancies, atoms at the edges interact with other edge atoms (next-nearest neighbors in the pristine lattice) which leads to the slight local atomic reconstructions^{6,13,14} and increases the corresponding T_d as compared to the edges of large vacancies. For displacing atoms at monovacancy edges, we obtained thresholds of $T_d^{B'} = 12.92$ eV and $T_d^{N'} = 15.00$ eV. For the edges of large vacancies (nine missing atoms), we obtained $T_d^{B\Delta} = 8.58$ eV and $T_d^{N\Delta} = 12.99$ eV. The ratio $T_d^{X'}/T_d^{X\Delta}$ of approximately 1.5/1.2 for $X=B/N$ is lower for both B and N than the experimental estimate, showing that in reality the ejection of atoms is faster for large defects than what would be directly expected from these values. The asymmetry in the ejection probabilities for B/N, which is at odds with the TB results,¹⁷ was earlier assumed to explain the experimental data.⁷ We stress, that although the T_d values were in the opposite order ($T_d^B > T_d^N$), the TB results¹⁷ gave the correct qualitative behavior at low voltages because the lower mass of B atom still lead to lower threshold voltage (74 kV as compared to 84 kV for N). However, these values predict the appearance of nitrogen monovacancies at voltages above 84 kV, contrary to the experiments.⁶

While charging has been proposed to be one of the factors effecting defect production in *h*-BN, we repeated the threshold calculations for the pristine structure and monovacancies in various charge states, Fig. 2(a). Negative/positive background was introduced to fulfill the electroneutrality condition. As evident from Fig. 2(a), for charged systems the T_d decrease. This result can be understood by analyzing bonding/antibonding orbital populations. The asymmetry between the thresholds for boron and nitrogen becomes lower. This suggests that charging is not likely to play an important role in the formation of the observed defects.

From T_d , one can estimate the displacement rate σ under known electron-beam conditions using the McKinley-Feshbach formalism for Coulombic scattering of relativistic electrons,²³ as described in Ref. 22. Although this model assumes an isotropic displacement energy, it gives a qualitative understanding of the relationship between T_d and σ , especially since the possible scattering angles due to momentum conservation for electron-atom scattering are very small (B/N are approximately 20,000 times heavier than electrons).

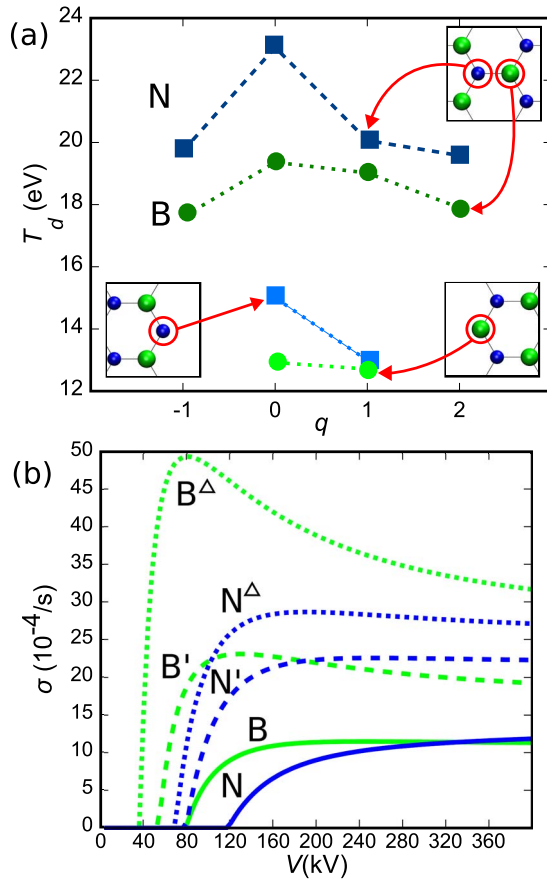


FIG. 2. (Color online) (a) Knock-on displacement thresholds for atoms in the pristine structure and for monovacancy edges as a function of the charge of the system q (total charge of the system). Squares denote the results obtained for nitrogen and circles for boron. (b) Displacement rates for B and N atoms in pristine structure (B/N), at monovacancy edges (B'/N'), and at edges of larger vacancies (B^Δ/N^Δ). These values were calculated for an electron-beam current of 10.0 A/cm^2 .

Note that in the experiments, the BN sheets are oriented essentially perpendicular to the electron beam. The calculated σ as a function of the acceleration voltage (electron-beam energy) are shown in Fig. 2(b). It is clear that σ for three-coordinated N atoms remains so low up to 120 kV that only boron monovacancies will appear, which explains ear-

lier experiments^{6,7} carried out at 80 and 120 kV. However, although nitrogen monovacancies would be expected to appear at voltages above 120 kV, based on the theoretical results, we were unable to unequivocally observe them in the experiments carried out at 200 kV. We believe that this is at least partly due to the complications arising from the rapid destruction of the target at this high voltage, which makes it difficult to obtain monolayer areas for comprehensive experiments via layer-by-layer sputtering. Other cause for the discrepancy could be chemical etching caused by impurities in the vacuum chamber. In any case, no mechanism in addition to knock-on damage is required to explain the experimental results at 80–120 kV.

For a direct comparison between the experimental and theoretical results, we developed a simulation code based on KMC. Our KMC model employs the displacement rates calculated from first principles. It assumes only one threshold energy per element for each coordination number (three, two). Atoms with only one neighbor are assumed to be immediately ejected since including a threshold for these atoms did not significantly alter the results. Examples of the structures obtained with the KMC code are presented in Fig. 3 for the three experimental acceleration voltages. A good agreement with the experimental results (Fig. 1) is observed, especially at lower voltages. It should be pointed out that our KMC method does not take into account the observed sudden changes in the atomic structure when growing vacancies approach each other and are separated only by narrow atomic bridges. This effect becomes more significant at higher voltages because of the increasing vacancy density. To partially compensate for this effect, we removed atoms in clusters which are loosely attached to the rest of the structure in Figs. 3(b) and 3(c). Obviously, for all voltages, both the experiment and the calculation strongly favor the triangle-shaped defect structures. However, the theoretically obtained multivacancies appear smaller and less defined than the experimental ones due to instabilities of the atomic structure, as mentioned above. The other possible explanation for the clean vacancy edges would be selective chemical etching, which we cannot completely exclude from the discussion, taking into account the vacuum level in our experiments (1×10^{-5} – 2×10^{-5} Pa). However, we stress that knock-on damage is sufficient to qualitatively describe the experimental observations. Simply from the ratio $\sigma^{B^\Delta}/\sigma^{N^\Delta}$ at 200 kV [Fig. 2(b)], as well as from Fig. 3, it is clear that the

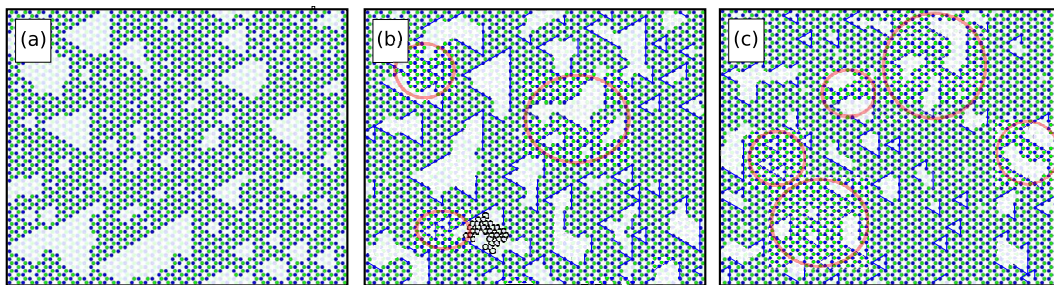


FIG. 3. (Color online) Results of kinetic Monte Carlo simulations corresponding to the experimental images shown in Fig. 1. Simulated acceleration voltages were (a) 80 kV, (b) 120 kV, and (c) 200 kV. Examples of removed atoms in unstable areas are shown with small circles, and large circles highlight areas where merging of vacancies could be expected to occur in a real experiment. Nitrogen-terminated edges are marked with lines in panels (b) and (c).

N-terminated edges appear more often than the B-terminated ones.

Taking into account the vacuum level in the chamber and possible passivation of dangling bonds with hydrogen atoms, we also checked what effect hydrogenation of vacancy edges would have on the displacement thresholds. Considering a triangular vacancy structure terminated by two-coordinated nitrogen atoms in the zigzag configuration, each nitrogen atom at the edge can form a bond with one hydrogen atom, which donates its electron to the nitrogen. The Bader charge analysis confirms that the edge N with an H has one electron more than the corresponding atom in the nonhydrogenated structure. The calculated thresholds show that H termination would stabilize the B edge more than the N edge, as the displacement thresholds increase almost by 3 eV for B but only about 0.5 eV for N at the edge of a vacancy. Hence, also H termination would lead to decreasing asymmetry between B and N edges, contrary to experimental results.

Because some of the experimental samples we used consisted of several layers, we also carried out calculations for bilayer and trilayer *h*-BN. Since *h*-BN is an ionic material, the interlayer description within DFT calculations can be expected to be more reliable than that for systems where only van der Waals interaction acts between the layers. We noticed a stabilizing effect (higher T_d) for B in a bilayer whereas N was always destabilized by the additional layers (lower T_d). Curiously, for a trilayer, the asymmetry between the B and N was slightly higher than for a monolayer. As a conclusion, the number of layers is not a decisive factor on creation of triangle-shaped vacancy defects in *h*-BN under TEM but the bilayer structure tends to be more radiation

resistant than monolayer or trilayer structures. This finding agrees well with our experimental results on the stability of few-layer *h*-BN under electron beam.

In conclusion, we combined multiscale atomistic simulations and HRTEM experiments to study the response of *h*-BN nanostructures to electron irradiation. We calculated the displacement threshold values for B/N atoms in pristine and defective *h*-BN systems in various charge states from first principles. Our results indicate that the picture based on the tight-binding values previously reported in the literature must be revised. In a perfect agreement with the experiments, our simulations show a high asymmetry between the thresholds for B/N, which explains the observed triangular multivacancy formation in *h*-BN under electron beam. Our findings also confirm the interpretation of N termination of edges of large triangle-shaped vacancy structures. Overall, our results attribute the formation of triangular-shaped multivacancies in *h*-BN monolayers to knock-on damage under the TEM. The presented microscopic mechanisms can be used for electron-beam engineering of BN nanostructures.¹¹ Further experiments using an environmental TEM could be used to estimate the role of etching in the process and assess the possibility of electron-beam-mediated substitution of B/N atoms with other chemical elements, e.g., carbon.²⁴

We thank CSC, Espoo, Finland for computer time through project IECBN09 and Academy of Finland for funding through project DEMECAN. The work on microscopy is partly supported by JST-CREST. C.H.J. also thanks the International Balzan Foundation for financial support through Meijo University.

-
- ¹D. Pacilé, J. C. Meyer, Ç. Ö. Girit, and A. Zettl, *Appl. Phys. Lett.* **92**, 133107 (2008).
- ²N. Alem, R. Erni, C. Kisielowski, M. D. Rossell, W. Gannett, and A. Zettl, *Phys. Rev. B* **80**, 155425 (2009).
- ³A. K. Geim and K. S. Novoselov, *Nature Mater.* **6**, 183 (2007).
- ⁴V. Barone and J. E. Peralta, *Nano Lett.* **8**, 2210 (2008).
- ⁵L. Ci *et al.*, *Nature Mater.* **9**, 430 (2010).
- ⁶C. Jin, F. Lin, K. Suenaga, and S. Iijima, *Phys. Rev. Lett.* **102**, 195505 (2009).
- ⁷J. C. Meyer, A. Chuvilin, G. Algara-Siller, J. Biskupek, and U. Kaiser, *Nano Lett.* **9**, 2683 (2009).
- ⁸C.-H. Park, F. Giustino, M. L. Cohen, and S. G. Louie, *Phys. Rev. Lett.* **99**, 086804 (2007).
- ⁹H. W. Zhang, S. Maiti, and G. Subhash, *J. Mech. Phys. Solids* **56**, 2171 (2008).
- ¹⁰A. V. Krasheninnikov and F. Banhart, *Nature Mater.* **6**, 723 (2007).
- ¹¹A. V. Krasheninnikov and K. Nordlund, *J. Appl. Phys.* **107**, 071301 (2010).
- ¹²W. Orellana and H. Chacham, *Phys. Rev. B* **63**, 125205 (2001).
- ¹³S. Azevedo, J. R. Kaschny, C. M. C. de Castilho, and F. de Brito Mota, *Nanotechnology* **18**, 495707 (2007).
- ¹⁴S. Okada, *Phys. Rev. B* **80**, 161404(R) (2009).
- ¹⁵L.-C. Yin, H.-M. Cheng, and R. Saito, *Phys. Rev. B* **81**, 153407 (2010).
- ¹⁶R. F. Egerton, P. Li, and M. Malac, *Micron* **35**, 399 (2004).
- ¹⁷A. Zobelli, A. Gloter, C. P. Ewels, G. Seifert, and C. Colliex, *Phys. Rev. B* **75**, 245402 (2007).
- ¹⁸G. Kresse and J. Furthmüller, *Phys. Rev. B* **54**, 11169 (1996).
- ¹⁹P. E. Blöchl, *Phys. Rev. B* **50**, 17953 (1994).
- ²⁰J. P. Perdew, K. Burke, and M. Ernzerhof, *Phys. Rev. Lett.* **77**, 3865 (1996).
- ²¹A. V. Krasheninnikov, F. Banhart, J. X. Li, A. S. Foster, and R. M. Nieminen, *Phys. Rev. B* **72**, 125428 (2005).
- ²²F. Banhart, *Rep. Prog. Phys.* **62**, 1181 (1999).
- ²³W. A. McKinley and H. Feshbach, *Phys. Rev.* **74**, 1759 (1948).
- ²⁴O. L. Krivanek, M. F. Chisholm, V. Nicolosi, T. J. Pennycook, G. J. Corbin, N. Dellby, M. F. Murfitt, Ch. S. Own, Z. S. Szilagy, M. P. Oxley, S. T. Pantelides, and S. J. Pennycook, *Nature (London)* **464**, 571 (2010).